High-frequency sea-level fluctuations recorded on a shallow carbonate platform (Berriasian and Lower Valanginian of Mount Salève, French Jura)

0012-9402/98/030375-16 $1.50 + 0.20/0
Birkhäuser Verlag, Basel, 1998

Eclogae geol. Helv. 91 (1998) 375–390

High-frequency sea-level fluctuations recorded on a shallow carbonate platform (Berriasian and Lower Valanginian of Mount Salève, French Jura)

ANDRÉ STRASSER[1] & HEIKO HILLGÄRTNER[1]

Key words: Jura Mountains, Berriasian, Valanginian, Carbonate platform, Sequence stratigraphy, Cyclostratigraphy, Sea-level changes

ABSTRACT

The Berriasian and Lower Valanginian strata of Mount Salève represent shallow-marine to peritidal sedimentary environments dominated by carbonates. Depositional sequences can be identified by a deepening-shallowing facies evolution. Periodic emersion is indicated by root horizons, calcrete, and black pebbles. Elementary sequences are the smallest units (usually beds) displaying such evolutions. They compose small-scale composite sequences again showing a transgressive-regressive facies trend. These stack into medium-scale composite sequences, which in turn build up large-scale sequences. Superposition of emersion features directly on subtidal facies and the good correlation of individual sequences over long distances suggest that relative sea-level fluctuations played an important role in sequence formation.

A 193-metre long, almost continuously exposed section is analysed in terms of sequence stratigraphy and cyclostratigraphy. Ten large-scale sequences have been identified. Due to superposition of high-frequency sea-level changes over a long-term trend, maximum-flooding zones and sequence-boundary zones commonly occur rather than well-expressed single surfaces. Biostratigraphic control by charophyte-ostracod assemblages, benthic foraminifera, and calpionellids allows to calibrate most large-scale sequence boundaries and to compare them with 3rd-order sequence boundaries of regional or global importance.

A repeated stacking of 2–6 elementary sequences into one small-scale sequence, and of 4 small-scale sequences into a medium-scale sequence is observed. At least 72 small-scale sequences making up 19 medium-scale sequences have been counted or are inferred from lateral correlation in the interval between 3rd-order sequence boundaries Be1 and Va1. Based on Gradstein et al. (1995), sequence boundary Be1 is dated at 144.2 (± 2.6) Ma by Hardenbol et al. (1998), sequence boundary Va1 at 136.5 (± 2.2) Ma. This general time framework and the hierarchical stacking pattern suggest that the formation of the depositional sequences was, at least partly, related to processes controlled by orbital cycles. The small-scale sequences may correspond to the 100-ky eccentricity cycle of the Earth's orbit, and the medium-scale sequences to the 400-ky eccentricity cycle. Thus, a time span of 7.2 to 7.6 my for the studied interval is implied by cyclostratigraphy (compared to 7.7 ± 4.8 my proposed by Hardenbol et al. 1998). The elementary sequences are interpreted to have formed in tune with the 20-ky cycle of precession of the equinoxes. However, because of low accommodation around large-scale sequence boundaries, not all elementary sequences have been recorded, and small-scale sequences may be condensed. During longer-term sea-level rises, the high-frequency sea-level drops were in many cases too attenuated to create elementary sequences. Late Cimmerian tectonic activity induced a major hiatus, but was not strong enough to mask the record of eustatic sea-level changes.

RESUME

Les sédiments d'âge Berriasien et Valanginien inférieur du Mont-Salève correspondent à des milieux de dépôt lagunaires à péritidaux dominés par des carbonates. Les séquences de dépôt sont définies par une évolution transgressive puis régressive des faciès. Traces de racines, calcrètes et galets noirs indiquent des émersions périodiques. L'unité la plus petite (en général un banc) qui démontre cette évolution est appelée séquence élémentaire. Les séquences élémentaires se groupent en petites séquences composites qui montrent également une évolution transgressive-régressive des faciès. Celles-ci se groupent en séquences moyennes, qui composent à leur tour de plus grandes séquences. La superposition d'indicateurs d'émersion sur des faciès subtidaux et la bonne corrélation des séquences sur de longues distances suggèrent que les fluctuations du niveau marin relatif jouaient un rôle important dans la formation de ces séquences.

Une coupe presque continue de 193 mètres d'épaisseur est analysée par les méthodes de la stratigraphie séquentielle et la cyclostratigraphie. Dix grandes séquences ont été identifiées. La superposition de fluctuations à haute fréquence sur une évolution du niveau marin à long terme induit la formation répétitive de surfaces qui définissent des zones de limite de séquence ou d'inondation maximale (plutôt que des surfaces uniques). Le contrôle biostratigraphique par foraminifères benthiques, calpionelles et assemblages charophytes-ostracodes permet de dater la majeure partie des limites de séquence et de les comparer avec celles d'importance régionale et globale.

On observe régulièrement un empilement de 2 à 6 séquences élémentaires qui forment une petite séquence, et de 4 petites séquences qui composent à leur tour une séquence moyenne. Au moins 72 petites séquences, groupées en 19 séquences moyennes, ont été comptées ou sont suggérées par corrélation latérale entre les limites de séquence de 3ème ordre Be1 et Va1. Se basant sur Gradstein et al. (1995), Hardenbol et al. (1998) datent la limite de séquence Be1 à 144,2 (± 2,6) Ma, Va1 à 136,5 (± 2,2) Ma. Ce cadre général de temps et l'agencement hiérarchique des séquences de dépôt suggèrent que leur formation était, au moins partiellement, en relation avec des processus contrôlés par les cycles orbitaux de la Terre. Une petite séquence pourrait correspondre au premier cycle d'excentricité de 100 ka, une séquence moyenne au deuxième cycle d'excentricité de 400 ka. Ainsi, l'analyse cyclostratigraphique indique une durée de 7,2 à 7,6 ma pour l'intervalle étudié (comparé à 7,7 ± 4,8 ma proposé par Hardenbol et al. 1998). Les séquences élémentaires se seraient formées en relation avec le cycle de précession des équinoxes de 20 ka. Cependant, parce que l'accommodation était faible autour des limites de séquence, une partie des séquences élémentaires ne pouvait pas être enregistrée et les petites séquences sont partiellement condensées. De même, lors d'une montée de niveau marin à long terme, les chutes du niveau marin à court terme étaient parfois trop faibles pour créer des séquences élémentaires. La phase tectonique tardi-cimmérienne provoquait un hiatus majeur mais n'était pas assez forte pour masquer l'enregistrement des fluctuations du niveau marin eustatique.

[1] Institut de Géologie et Paléontologie, Pérolles, CH–1700 Fribourg
E-mail andreas.strasser@unifr.ch

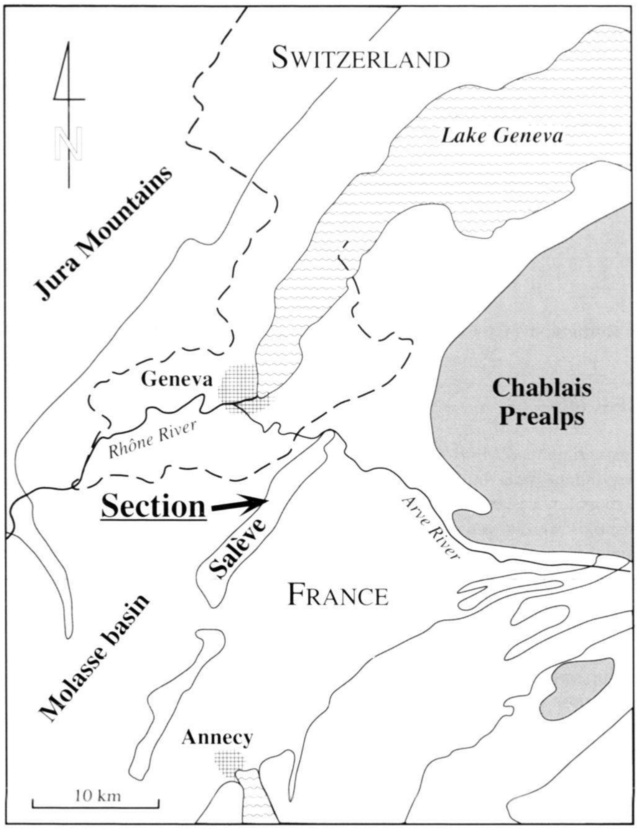

Fig. 1. Location of studied section.

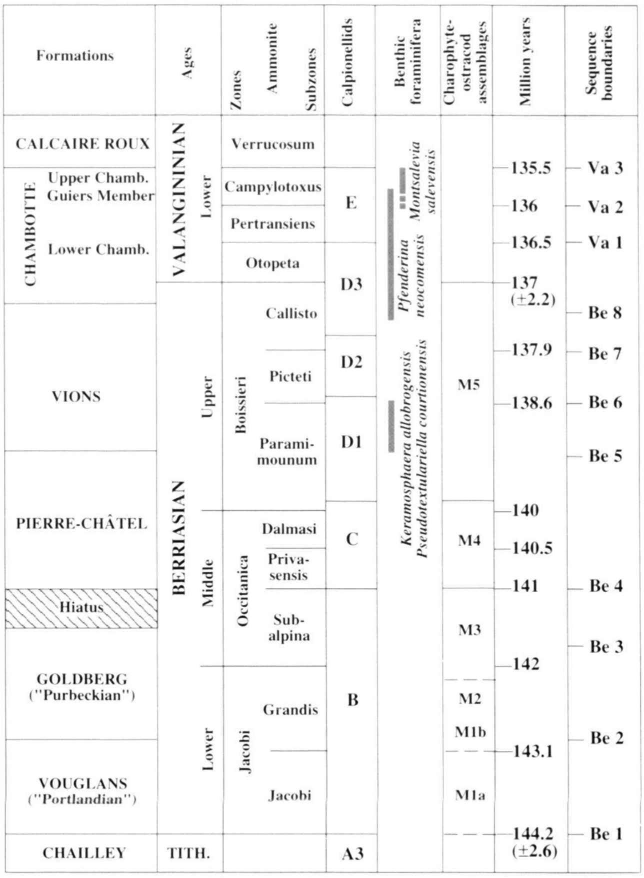

Fig. 2. Chronostratigraphic and sequence-stratigraphic position of the studied formations. Ammonites after Le Hégarat & Remane (1968) and Le Hégarat (1971, 1980), calpionellids after Remane (1985), position of benthic foraminifera after Clavel et al. (1986) and Blanc (1996), charophyte-ostracod assemblages after Mojon (in Détraz & Mojon, 1989). Ages of ammonite subzone boundaries and 3rd-order sequence boundaries after Hardenbol et al. (1998), based on Gradstein et al. (1995).

Introduction

Situated between the Jura Mountains and the Subalpine Chains, Mount Salève rises from the Molasse Basin just southeast of the city of Geneva (Fig. 1). It constitutes the frontal part of a thrustsheet that has been moved northwestwards over the Lower Freshwater Molasse of Late Oligocene age (Gorin et al. 1993). The steep, west-northwest facing cliffs exhibit an exceptionally well-exposed and almost continuous sedimentary succession spanning the Upper Kimmeridgian to Lower Barremian interval (Lombard 1967). The stratigraphy of Mount Salève has been described in great detail by Joukowsky & Favre (1913) early in this century, and Maillard studied its Purbeckian facies already in 1884. Carozzi (1948, 1953, 1954, 1955) and Lombard (1976) added details about the sedimentology and microfacies. Interpretations of the stratal stacking pattern in the Portlandian and Purbeckian were given by Strasser (1988a). Deville (1991) presented a comprehensive stratigraphic and sedimentological study of the mountain.

The section analysed in this paper begins at the base of a cliff, at the intersection of Chavardon and Etiollets trails, and follows the very steep and rocky Etournelles trail uphill. It crosses the Corraterie trail and ends close to the Trou de la Tigne, where the cliffs give gradually way to the meadow covering the top of the mountain. The outcrop is almost continuous, and the strata are horizontal where the section has been measured. The section comprises the Portlandian Tidalites-de-Vouglans Formation (Bernier 1984), the Goldberg Formation ("Purbeckian"; Häfeli 1966), and the Pierre-Châtel, Vions and Chambotte Formations (Steinhauser & Lombard 1969), thus covering the Berriasian and the lowermost part of the Valanginian (Fig. 2). Biostratigraphic dating in the lower part of the section is poor, and the chronostratigraphic framework there has to be strengthened through lateral correlation of well-defined lithological boundaries.

The section is interpreted in terms of high-resolution sequence stratigraphy and cyclostratigraphy. By applying the sequence-stratigraphic concepts (e.g. Posamentier et al. 1988; Handford & Loucks 1993) also to small depositional se-

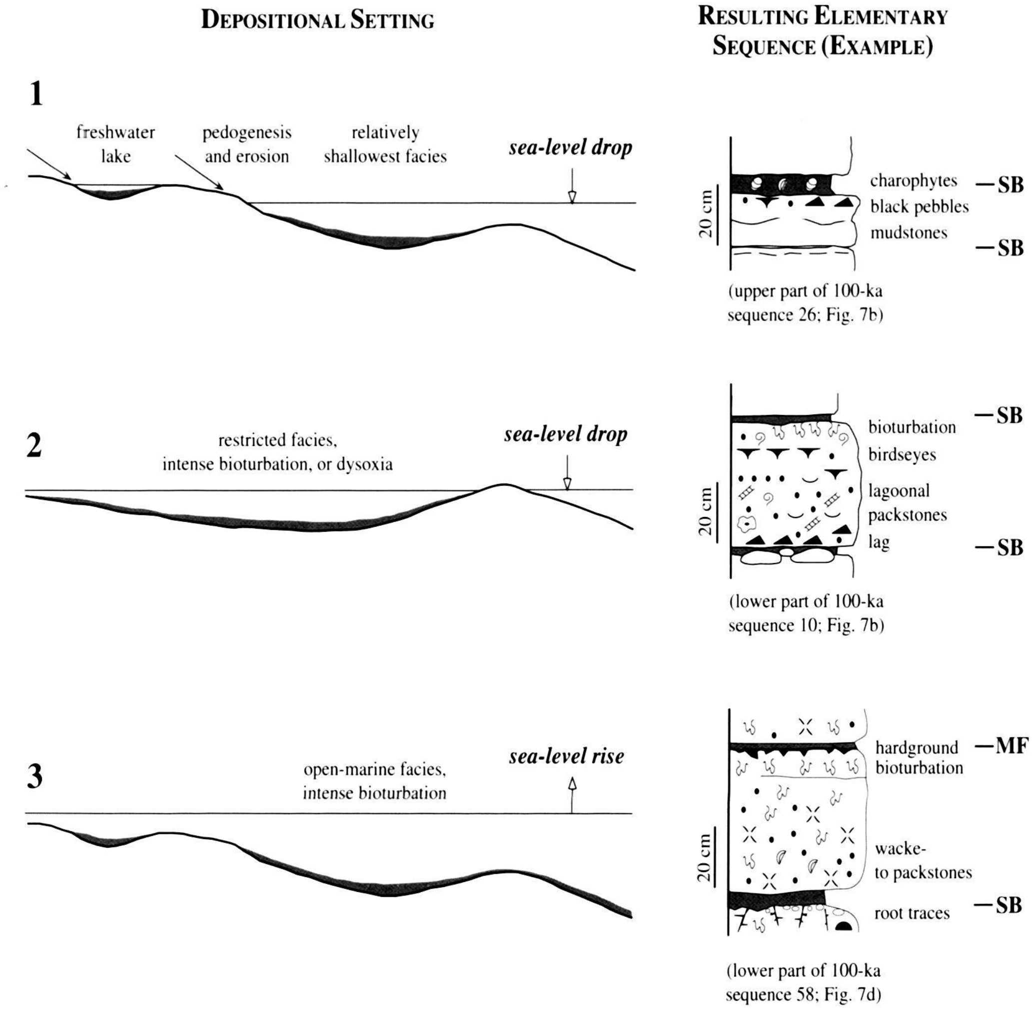

Fig. 3. Different models for clay occurrence, which commonly defines bedding planes. Examples of elementary sequences are taken from the studied section. For discussion refer to text. Legend is given in Fig. 4.

quences, a better understanding of the depositional processes related to changes in accommodation potential, carbonate production, and sediment supply can be reached (Schlager 1993). In order to place these processes in a narrow time framework, a cyclostratigraphical analysis of the observed hierarchical stacking of depositional sequences is attempted.

Definition of depositional sequences and high-resolution sequence stratigraphy

The facies encountered in the studied section represent tropical to subtropical depositional environments: shallow lagoons, ooid shoals, high-energy beaches, tidal flats, sabkhas, lakes, and isolated islands (Strasser 1988b; Deville 1991). The facies evolutions on the scale of individual beds and bed sets commonly imply first a deepening, then a shallowing of depositional conditions, and/or a change from rather restricted to more open-marine and back to restricted conditions (Strasser 1991). These facies evolutions are punctuated by surfaces pointing to submarine erosion, condensation, subaerial exposure, or to rapid facies changes (Hillgärtner 1998a). The sedimentary package contained between two such surfaces is called a depositional sequence.

Formation of diagnostic surfaces

Many bedding surfaces observed in the outcrop are accentuated by differential weathering of marly layers, implying increased clay content. Occurrence of clay can be related to four main factors (Fig. 3):

1. *Rapid fall of relative sea level* increases the erosion potential in the hinterland and thus clay input into the shallow-marine realm. Accordingly, the clays are associated with

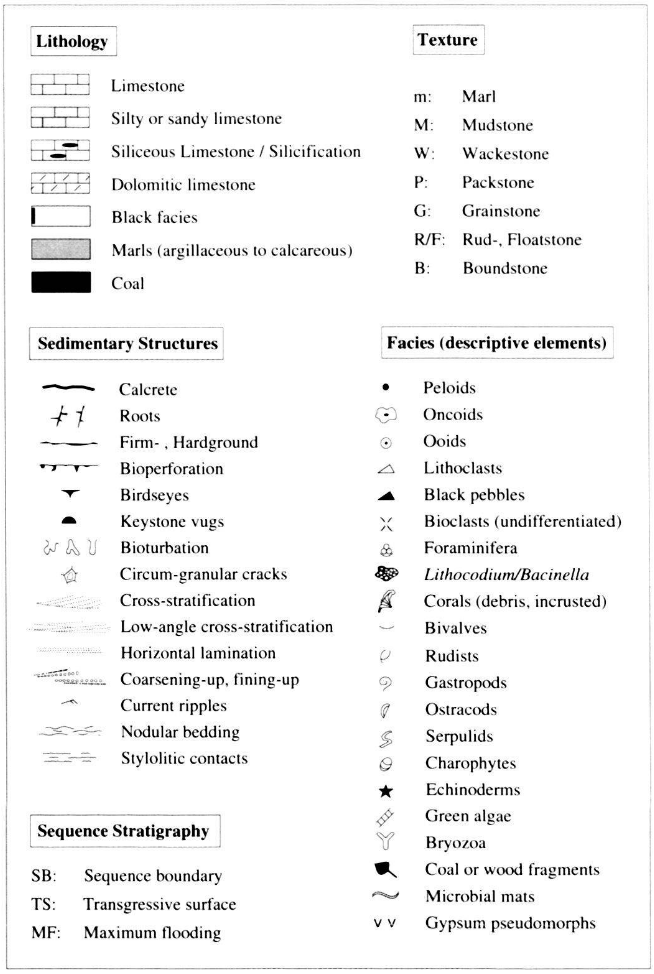

Fig. 4. Legend for the detailed sections in Figs 3, 5 and 7.

the shallowest or most restricted facies. In the case of the "Portlandian" and "Purbeckian", green clays rich in neoformed illite are related to alternating wetting and drying in marginal-marine settings (Deconinck & Strasser 1987). Charophytes and fresh-water ostracods occur in some of these marls and indicate local freshwater lakes on the shallow, partly emergent platform (Mojon & Strasser 1987). Black pebbles point to emersion and, locally, to forest fires (Strasser & Davaud 1983). Depositional sequences contained between such marly layers correspond to the "simple sequences" of Vail et al. (1991), which are bounded by sequence boundaries.

2. Low-energy conditions on the platform result in the settling out of the clays. This situation may be related to *low sea level that isolates pools and shallow lagoons* from the open-marine influence. In this case, the marly layers exhibit restricted fauna and increased density of bioturbation due to lowered sedimentation rates, or dysoxic facies due to reduced water circulation. The marly layers again are associated with sequence boundaries.
3. Low-energy conditions can also be created by *rapidly rising sea level* (transgressive pulses or maximum flooding in the sequence-stratigraphic sense; Vail et al. 1991), which positions the sea floor below wave base. These marly layers are characterized by a relatively open-marine fauna, facies is relatively deep, and bioturbation density may be high due to low sedimentation rates. In this case, the beds visible in the field are bounded by marine flooding surfaces (including the maximum-flooding surface) and thus correspond to "parasequences" in the sense of Van Wagoner et al. (1990), or to the "subtidal cycles" of Osleger (1991).
4. *Increased rainfall* in the hinterland also increases clay input into the marine system. Such climatic changes depend on palaeolatitude and atmospheric circulation patterns and can occur at any time of a sea-level cycle (Perlmutter & Matthews 1989; Pittet & Strasser 1998). In certain palaeogeographic positions and palaeoclimatic regimes, climate may be more humid at high sea-level stands and will favour the formation of "parasequences", in other contexts more rain occurs at low sea levels, helping the formation of "simple sequences".

Formation and stacking of these sequences can best be explained by periodically changing accommodation on the shallow carbonate platform. The potential of carbonate production is high, and the mostly organically produced sediment can rapidly fill up the available space created by relative sea-level rise. Slowing sea-level rise or a drop then leads to emersion, reworking, and early fresh-water diagenesis, thus defining the boundary of a small-scale sequence (Strasser 1994; D'Argenio et al. 1997). Stable-isotope analyses point to evaporation and to soil gas influencing diagenesis in the upper part of the subaerially exposed sequences (Joachimski 1994). The fact that the tops of many small-scale sequences show emersion features, erosion, intertidal overprinting of subtidal facies and, in several cases, calcrete caps and/or root traces, suggests that sea-level fluctuations played an important role in the formation of these sequences. Such features cannot be created only by progradation of tidal flats (Ginsburg 1971) or migrating lobes and channels (Pratt & James 1986), but imply a fall of sea level below the sediment surface (Strasser 1991). When space becomes available again through renewed relative sea-level rise, and after a certain lag time during which pre-existing material is reworked, carbonate production and accumulation starts again, and a new sequence is deposited. If sea-level fluctuations are composed of different cyclicities with varying frequencies and amplitudes, the resulting stacking pattern of small-scale depositional sequences will display an equally complex hierarchy (e.g., Mitchum & Van Wagoner 1991; Goldhammer et al. 1990, 1994; Montañez & Osleger 1993; D'Argenio et al. 1997).

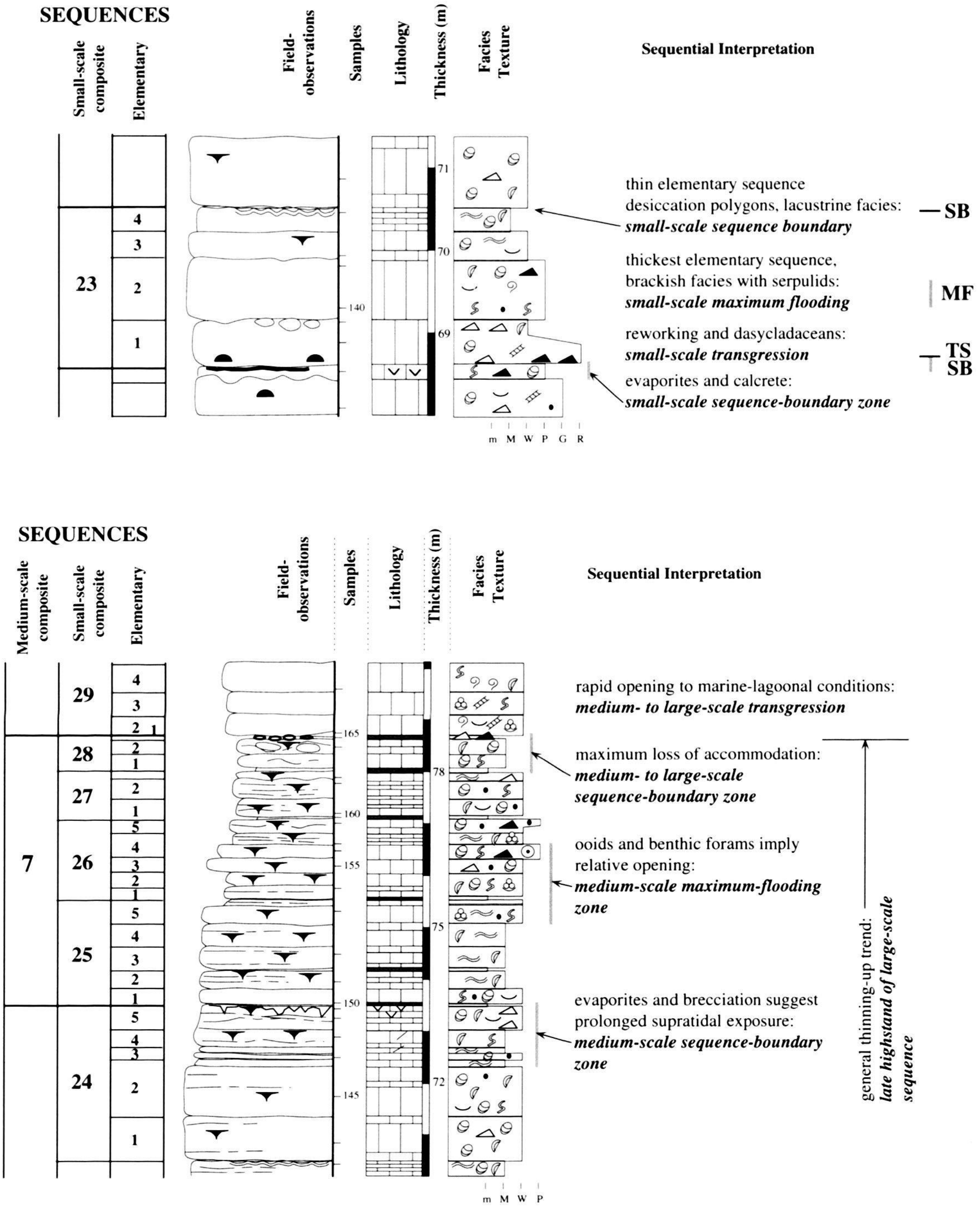

Fig. 5. Examples of stacking of depositional sequences. For discussion refer to text. Numbers of sequences correspond to those in Fig. 7. The legend is given in Fig. 4.

Types of depositional sequences

In the section studied at Mount Salève, four orders of depositional sequences have been recognized:

1. *Elementary sequences* are the smallest units recognizable in the field. They commonly correspond to one bed. Transgressive-regressive trends of facies evolution can be identified in many cases, but also beds with homogeneous facies distribution occur. Some of these elementary sequences may have formed through autocyclical processes such as lateral migration of tidal channels or shifting of carbonate shoals (Pratt & James 1986; Strasser 1991). Elementary se-

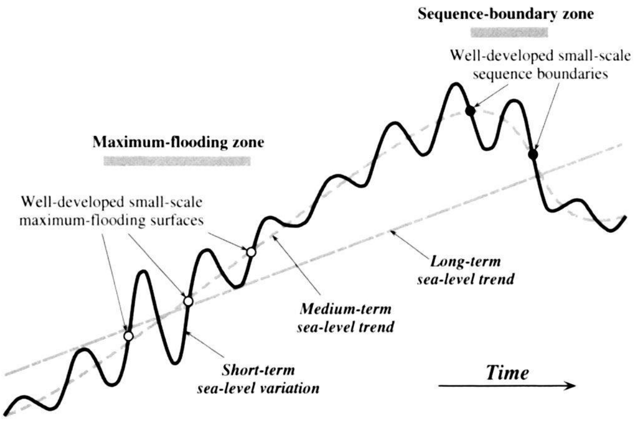

Fig. 6. Superposition of high-frequency sea-level fluctuations on longer-term sea-level trends leads to multiplication of diagnostic surfaces, where maximum-flooding zones or sequence-boundary zones can be defined. High amplitude of the high-frequency fluctuation enhances the expression of a diagnostic surface. Longer-term sea-level rises enhance small-scale maximum-flooding surfaces, longer-term sea-level drops lead to a better expression of small-scale sequence boundaries.

quences range in thickness from a few centimetres to a few metres.

2. *Small-scale (composite) sequences* are built up by 2–6 elementary sequences. They generally show a well-defined transgressive-regressive facies evolution (Fig. 5). Many of these sequences can be interpreted in terms of sequence stratigraphy. After flooding of the previously exposed substrate and partly reworking it, accommodation increases during a relative sea-level rise, but carbonate production is still low. Transgressive depositional environments such as tidal flats or beaches are quickly drowned, and lagoonal conditions prevail. Water depth now is ideal for maximum carbonate production (Tipper 1997), which gradually fills up the available space. This is when the thickest beds are created, corresponding to the phase of maximum flooding. A distinct maximum-flooding surface is not necessarily developed. Highstand deposits then thin upward, and emersion features become more abundant towards the top of these sequences. A sequence boundary marks the end of this evolution. Due to the generally very shallow depositional environments and lacking accommodation, lowstand deposits are very thin or not developed at all. Thus, transgressive surfaces coincide in many cases with the sequence boundaries. Around the sequence boundaries, the elementary sequences may contain surfaces pointing to maximum regression. Sequence boundaries thus may be doubled or tripled, which is due to the superposition of a high-frequency fluctuation of relative sea level over a lower-frequency sea-level trend (Montañez & Osleger 1993; Pasquier & Strasser 1997). Similarly, transgressive or maximum-flooding surfaces may be multiplied. Intervals of repeated surfaces are defined as sequence-boundary zones, transgressive-surface zones, or maximum-flooding zones (Figs 5 and 6). The observed small-scale composite sequences are a few tens of centimetres to a few metres thick.
3. *Medium-scale (composite) sequences* are generally composed of 4 small-scale sequences. Facies evolution, repetition of diagnostic sequence-stratigraphic surfaces, and definition of sequence-boundary and maximum-flooding zones are comparable to those of the small-scale composite sequences. Medium-scale composite sequences measure from a few metres to a few tens of metres (example in Fig. 5).
4. *Large-scale (composite) sequences* are the largest units that have been recognized in the studied section. These sequences are comparable to the 3rd-order sequences of Vail et al. (1991), which are related to longer-term (million-year scale) changes of relative sea level. They show well-developed sequence-boundary and maximum-flooding zones. Their facies evolution and ages will be discussed below.

On all scales, most of the observed depositional sequences shallow upwards into very shallow subtidal, intertidal or supratidal facies (Figs 5 and 7). This indicates that the space created by subsidence and sea-level rise has been filled in most cases. Changes in (decompacted) thicknesses of the depositional sequences therefore very roughly translate changes of accommodation through time. However, in order to reconstruct sea-level changes with Fischer plots (e.g., Read & Goldhammer 1988) or perform statistical analyses (e.g., Bond et al. 1993), each individual sequence would have to be decompacted (using different factors dependent on facies), the depth of the vadose zone would have to be evaluated, and the potentially eroded sediment thickness would have to be estimated. Furthermore, the same time duration would have to be attributed to each type of sequence, and subsidence would have to be assumed to be constant throughout the studied interval. It is outside the scope of the present paper to reconstruct a relative sea-level curve, or to mathematically analyse the periodicities of the stacked sequences.

Facies evolution, biostratigraphy, and long-term sequence-stratigraphic interpretation

Tidalites-de-Vouglans Formation

The thick-bedded oncoidal grainstones at the base of the section (Fig. 7a) belong to the uppermost part of the Calcaires-coralliens-des-Etiollets Formation (Deville 1991), which corresponds to the Couches-de-Chailley Formation of Bernier (1984). The limit to the Tidalites-de-Vouglans Formation (Bernier 1984) has been set where an erosive surface cuts into the underlying oncoidal packstone. The overlying small-scale composite sequence (1) composed of 4 to 5 beds displays a shallowing-upward trend, going from subtidal channel-fill deposits with black pebbles and some charophytes to dolomitized algal-microbial mats. The following small-scale sequence (2) is dominated by lacustrine facies and also contains coalified plant fragments. This rapid change of accommodation and facies is attributed to a drop of relative sea level on the longer term; correlation with other outcrops in the French Jura Mountains permits to identify it as sequence boundary Be1 of at least regional importance (Strasser 1994; Hardenbol et al. 1998). Precise biostratigraphic dating of this sequence boundary at Mount Salève is not possible (Deville 1991).

Many of the following small-scale composite sequences (3–16) begin with lagoonal facies including echinoderms, dasycladacean algae and oncoids, and commonly grade up into thin beds with fenestral biomicrites or dolomitized algal mats. Conglomerates at the base of some small sequences point to reworking due to flooding of a previously consolidated emersion surface. The interval of fastest creation of accommodation (maximum flooding) related to the longer-term sea-level evolution can be placed where the individual beds and the small-scale composite sequences are thickest (sequence 4, Fig. 7a). At the level of the upper cave, pebbles of calcrete indicate prolonged subaerial exposure (Fig. 7b). Individual beds and small-scale sequences generally become thinner and show more restricted facies, suggesting that accommodation space on the platform is being gradually reduced. This evolution corresponds to a highstand on the longer-term sea-level evolution.

An interval of about 1 metre showing many well-developed emersion features includes the top of small-scale sequence 16 and sequence 17 (Fig. 7b). Polygonal mudcracks, beachrock slabs of oosparite and an up to 4 cm-thick calcrete crust can be followed over tens of metres along the cliff. This interval correlates with similar ones in other sections of the Swiss and French Jura (Strasser 1994) and is interpreted as a 3rd-order sequence boundary (possibly Be2, but see discussion below). It also marks the limit between the Tidalites-de-Vouglans Formation and the Goldberg Formation (Häfeli 1966).

Goldberg Formation

The Goldberg Formation exhibits the typical Purbeckian facies: restricted lagoonal and intertidal biopelmicrites with abundant fenestrae, lacustrine charophyte- and ostracod-bearing micrites, algal-microbial laminations locally including evaporite pseudomorphs, green marls and black pebbles some of which have been blackened by forest fires (Strasser & Davaud 1983). The beds are generally thin, implying a low accommodation potential. Charophyte-ostracod assemblages (M1b of Mojon 1988 and Détraz & Mojon 1989) suggest an age corresponding to the Grandis Subzone of the lowermost Berriasian. A 3rd-order sequence boundary (Be3) has been placed at the top of small-scale sequence 28 (Figs 5 and 7b).

Small-scale sequence 29 displays relatively thick beds and contains more open-lagoonal facies with dasycladaceans, suggesting a slight transgressive phase on the long-term trend of sea-level evolution. The overlying beds (small-scale sequences 30 to 32) are mostly mudstones and wackestones rich in birdseyes, again pointing to a general decrease in accommodation.

The top of the Goldberg Formation shows evidence of non-deposition, erosion, and reworking (Fig. 7b). Individual beds and sequences pinch out laterally, but at least 4 severely reduced small-scale sequences can be inferred (Strasser 1988b, 1994). Correlation with other sections in the French and Swiss Jura, which have been dated by charophyte-ostracod assemblages (P.-O. Mojon, pers. comm.) and by ammonites (Clavel et al. 1986), indicates that the Subalpina Subzone is missing or strongly condensed at Mount Salève. The top of the Goldberg Formation thus represents an important sequence boundary (Be4) related to the long-term evolution of sea level and, probably, tectonic activity (see discussion below).

Pierre-Châtel Formation

The overlying Pierre-Châtel Formation (Steinhauser & Lombard 1969) is dated as Middle Berriasian by ammonites and begins in the Privasensis Subzone (Deville 1991). Oosparites with well-marked foresets imply that a sandwave migrated rapidly over the intertidal to emersive Purbeckian sediments; echinoderms suggest a fully marine environment (Fig. 7c). Accordingly, the base of the Pierre-Châtel Formation corresponds to an important transgressive surface, which can be correlated regionally.

The top of the Formation was originally defined by the change to reddish, mixed siliciclastic-carbonate lithologies of the Vions Formation (Steinhauser & Lombard 1969). With better biostratigraphic constraints it is now placed at the first appearance of "*Keramosphaera*" *allobrogensis*, a large benthic foraminifer attributed to the Paramimounum Subzone (Clavel et al. 1986). "*K.*" *allobrogensis* STEINHAUSER, BRÖNNIMANN & KOEHN-ZANINETTI is the type species of *Pavlovecina* LOEBLICH & TAPPAN, n.gen. (Loeblich & Tappan 1988).

The lower two thirds of the Pierre-Châtel Formation show open-marine and predominantly high-energy facies corresponding to alternating oolite shoals and open lagoons. The generally thick-bedded limestones indicate high accommodation, which implies an important transgressive phase on the long-term sea-level evolution. Small intervals of thinner-bedded and/or intensely bioturbated sediments of a lagoonal facies (sequences 39, 40, and 43, Fig. 7c) indicate condensation in small-scale composite sequences. Above about one metre of covered section (sequence 44, Fig. 7c), an abrupt change to tidal-flat and restricted-lagoonal facies takes place. The overlying interval, around 5 metres thick, is covered again. Some beds outcropping in the steep grassy hillside show tidal-flat facies with birdseyes. Correlation with a fully exposed section nearby indicates that this lithology continues all the way up to sequence boundary Be5 that is, without doubt, located somewhere in the covered interval in the Salève section. This regionally important surface is marked by a karst over wide areas of the Jura Mountains (Pasquier 1995). Comparison of the general evolution of this section with that of other sections in both platform and basin settings implies that the 3rd-order highstand deposits are relatively thin and may locally be eroded (Pasquier & Strasser 1997).

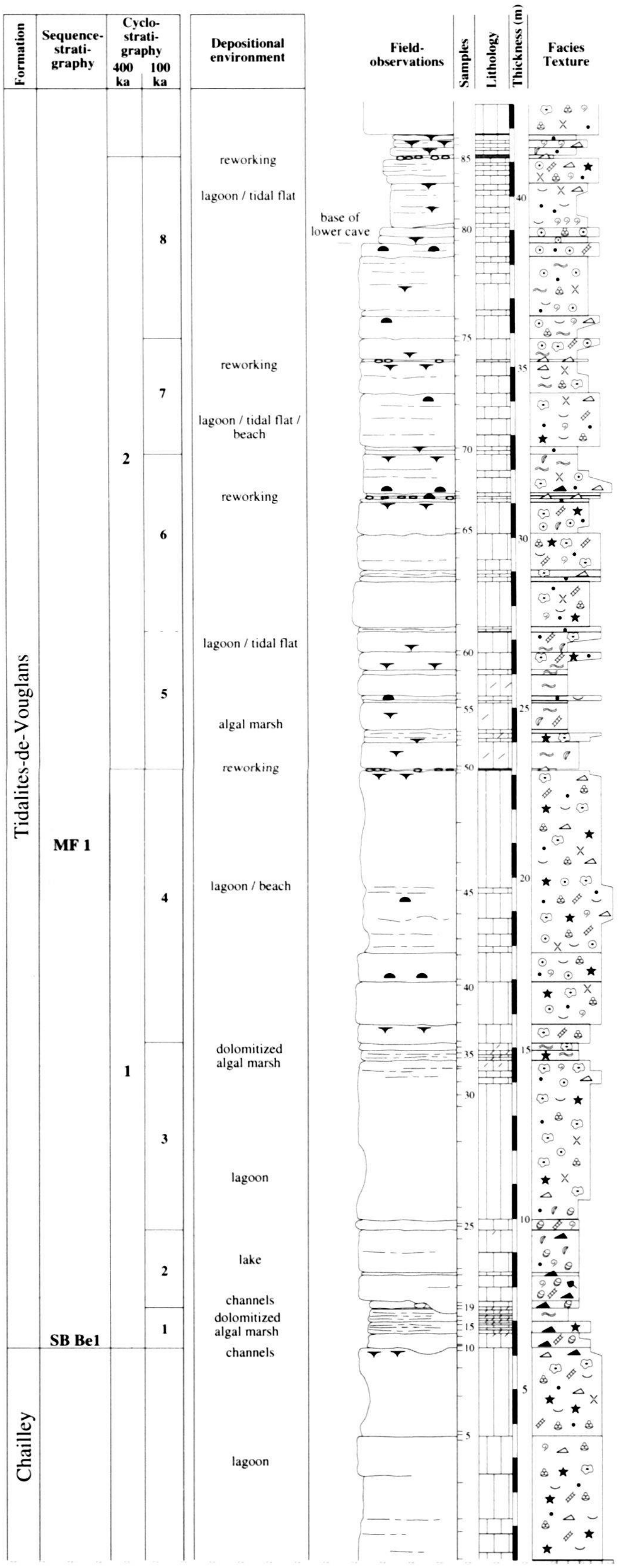

Formation
Sequence-stratigraphy
Cyclo-stratigraphy
400 ka
100 ka
Depositional environment
Field-observations
Samples
Lithology
Thickness (m)
Facies Texture
Tidalites-de-Vouglans
Chailley
MF 1
SB Be1
reworking
lagoon / tidal flat
base of lower cave
reworking
lagoon / tidal flat / beach
reworking
lagoon / tidal flat
algal marsh
reworking
lagoon / beach
dolomitized algal marsh
lagoon
lake
channels
dolomitized algal marsh
channels
lagoon
mMWPGR

Fig. 7a

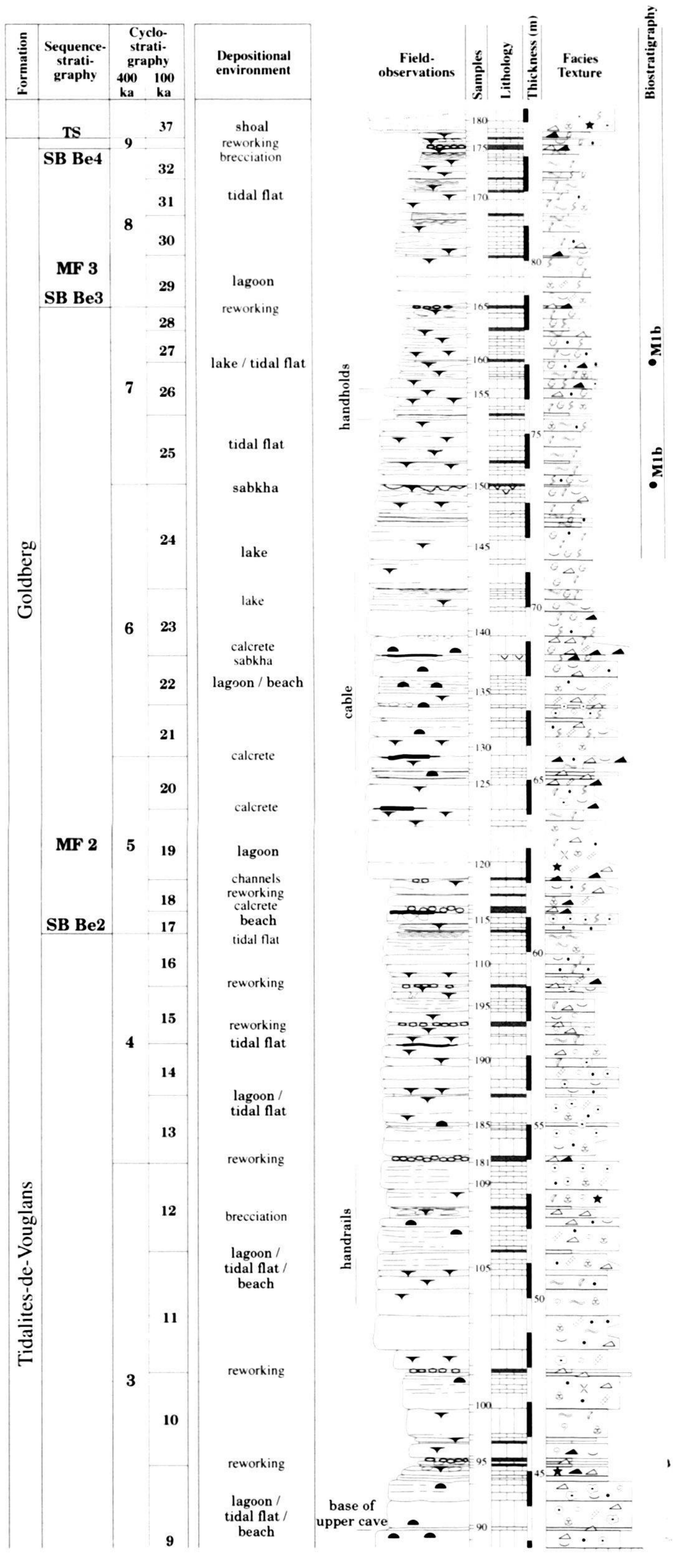

Formation
Sequence-stratigraphy
Cyclo-stratigraphy
400 ka
100 ka
Depositional environment
Field-observations
Samples
Lithology
Thickness (m)
Facies Texture
Biostratigraphy
Goldberg
Tidalites-de-Vouglans
TS
SB Be4
MF 3
SB Be3
MF 2
SB Be2
shoal
reworking
brecciation
tidal flat
lagoon
reworking
lake / tidal flat
tidal flat
sabkha
lake
lake
calcrete
sabkha
lagoon / beach
calcrete
calcrete
lagoon
channels
reworking
calcrete
beach
tidal flat
reworking
reworking
tidal flat
lagoon / tidal flat
reworking
brecciation
lagoon / tidal flat / beach
reworking
reworking
lagoon / tidal flat / beach
handholds
cable
handrails
base of upper cave
M1b
M1b
mMWPGR

Fig. 7b

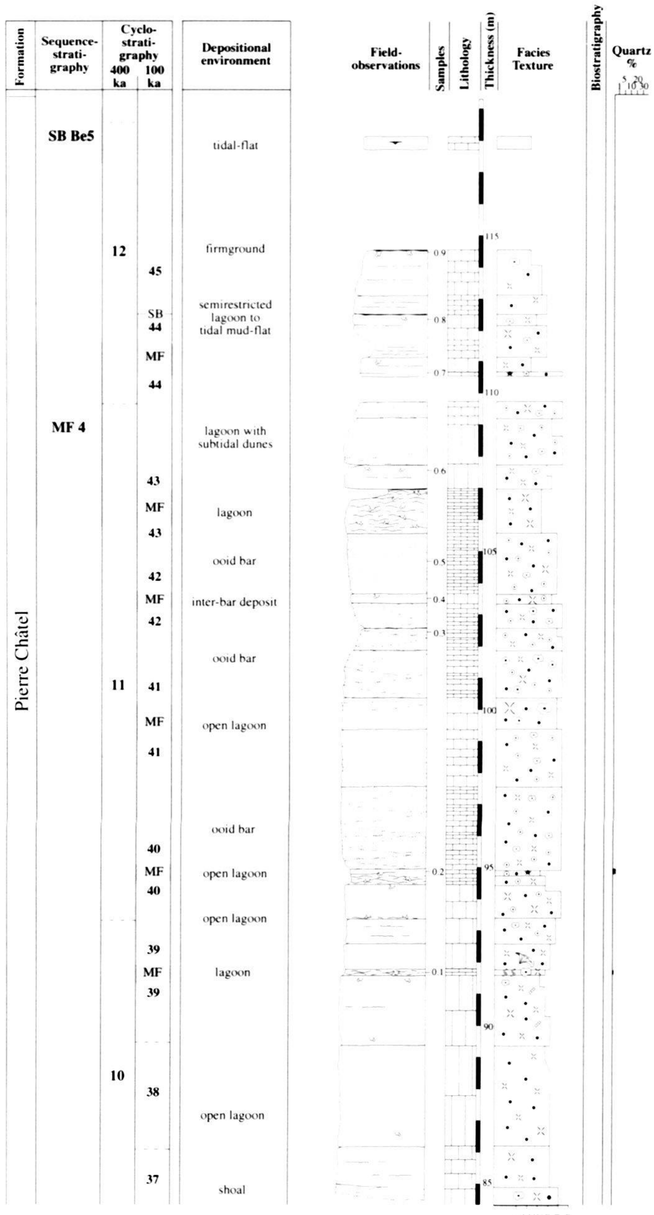

Fig. 7c

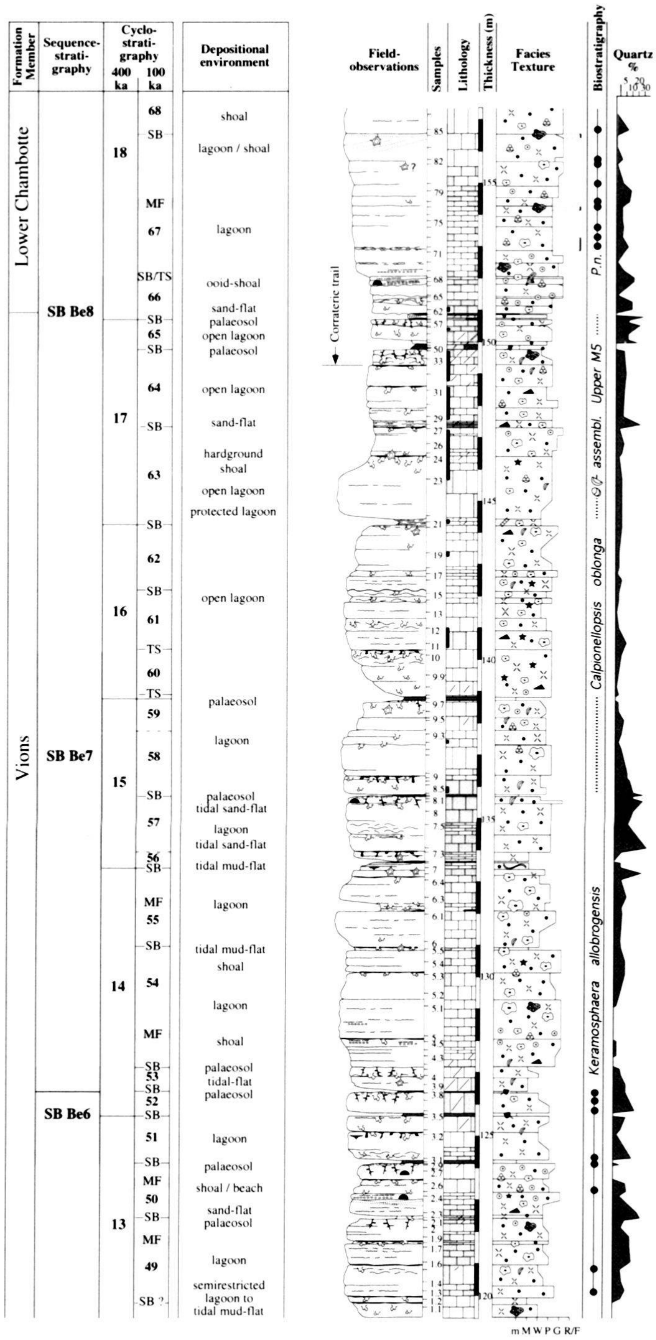

Fig. 7d

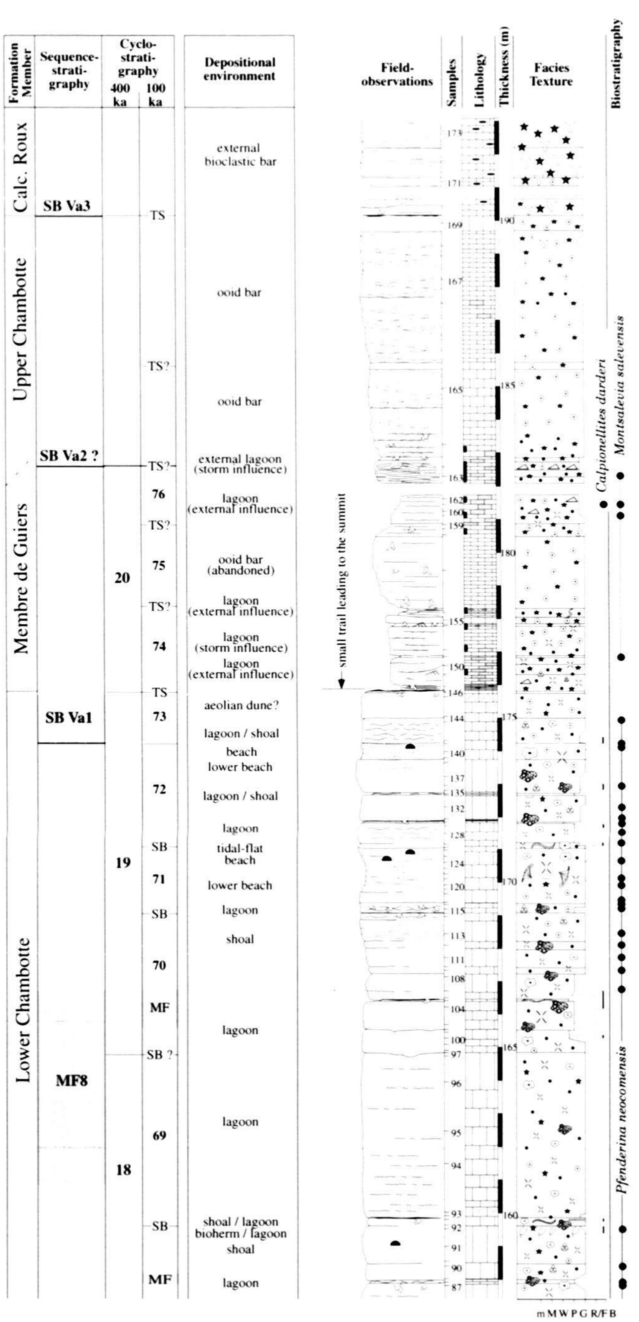

Fig. 7e

Fig. 7a–e. Studied section at Salève Mountain. For discussion and interpretation refer to text. Legend in Fig. 4.

Vions Formation

The Vions Formation is biostratigraphically well dated. *"Keramosphaera" allobrogensis* at the base indicates the Paramimounum Subzone (Fig. 2). *Calpionellopsis oblonga* (calpionellid Zone D2) found in the lateral equivalents of sequences 58 and 59 (Zaninetti et al. 1988; Deville 1991) is attributed to the Picteti Subzone. Close to the top of the Formation, ostracod assemblages indicate the upper M5 zone of Détraz & Mojon (1989) corresponding to the Callisto Subzone (uppermost Berriasian; Deville 1991).

Characteristic of the Vions Formation are its quartz content (Fig. 7d) that in some beds reaches up to 30%, and its reddish colour caused by oxidation of pyrite. Many of the well stratified, relatively thin beds show intense bioturbation *(Thalassinoides)*, indications of firm- and hardgrounds, as well as numerous palaeosol horizons. Facies imply open lagoons with local shoals and tidal flats. Relatively low accumulation rates are assumed, which however kept pace with relative sea-level rise on the long term. Small-scale sea-level falls therefore rapidly led to subaerial exposure.

The base of the Vions Formation is marked by lagoonal sedimentation and abundant bioturbation. Then follow several horizons with palaeosols. A zone of repetitive emersion, represented by three small-scale composite sequences (51 to 53, Fig. 7d), can be correlated over wide areas of the platform (Hillgärtner 1998b). Regionally, the palaeosol horizon on top of sequence 52 is the best-developed one and coincides with the abrupt disappearance of *"Keramosphaera" allobrogensis*. It is the best candidate for the widely recognized sequence boundary Be6 (Hardenbol et al. 1998).

The facies evolution then indicates a short opening with high-energy shoals and open lagoons (Fig. 7d). Important emersive facies occur again in sequences 55 to 57. The regional importance of the palaeosol horizons and the age of this interval (calpionellid Zone D2 - Picteti Subzone) allow to attribute this interval to sequence boundary Be7. However, the following 3 metres of the section show several emersions, which probably represent a multiplication of sequence boundaries on the scale of small-scale composite sequences, related to this long-term regressive evolution. Maximum regression at this sequence-boundary zone is observed regionally (Hillgärtner 1998b). In sequence 63, two thick beds indicate a short-lived high accommodation, which gradually decreases towards the top of the Formation. Palaeosols and coal beds (sequences 65 and 66, Fig. 7d) again mark a relative sea-level fall in the Callisto Subzone, attributed to sequence boundary Be8.

Chambotte Formation

The overlying, massive white limestones just below the top of Mount Salève belong to the Lower Chambotte Member. The abrupt change to high-energy facies and high accommodation potential mark a regionally synchronous transgressive trend (Fig. 7e). The benthic foraminifer *Pfenderina neocomensis* PFENDER indicates a latest-Berriasian to Early-Valanginian age (upper Callisto, Otopeta, and Pertransiens Zones; Deville 1991, Blanc 1996).

The base of the Member is dominated by oolite shoals, which locally show vadose cementation (Fig. 7d). Lagoonal sediments (sequences 69 and 70; Fig. 7e) indicate highest accommodation and a maximum flooding on the longer-term evolution of sea level. Small-scale composite sequences are generally less well marked than in the Vions Formation, probably due to the intrinsic dynamics of the high-energy sedimentary environments. The uppermost, thinner-bedded sediments of the Lower Chambotte Member again represent high-energy shoal to coarse beach deposits. The top of sequence 72 showing vadose cementation is a good candidate for 3rd-order sequence boundary Va1. A distinct surface with encrusting bivalves and bioerosion marks the top of the Member and is interpreted as a superposition of a small-scale sequence boundary by a major transgressive surface marking the onset of sedimentation on the external platform. The fact that the transgressive surface is better marked than the sequence boundary indicates a general transgressive trend (Fig. 6), probably on a 2nd-order scale (Haq et al. 1987).

The following yellowish, echinoderm-rich, oolitic limestones with a weak siliciclastic content are attributed to the Guiers Member. The assemblage of *Tintinnopsella carpathica* (MURGEANU & FILIPESCU) and *Calpionellites darderi* (COLOM) (calpionellid Zone E) found by Deville (1991) are characteristic of the Pertransiens to Campylotoxus ammonite zones (Lower Valanginian; Fig. 2). The benthic foraminifer *Montsalevia salevensis* CHAROLLAIS, BRÖNNIMANN & ZANINETTI appears in the lower part of the Campylotoxus Zone (according to Blanc 1996, but in its middle part according to H. Arnaud, pers. comm.). Small-scale composite sequences in the Guiers Member are different from those observed in the formations below. Typically, their base is made up of echinoderm-rich sediments passing into oolitic grainstones showing hummocky cross-stratification (sequence 76). They are interpreted as "subtidal cycles" (Osleger 1991) where the base indicates deposition below storm-wave base during rapid relative sea-level rise. Their upper part, influenced by storms, indicates sedimentation during slowing relative sea-level rise and relative sea-level fall. Major reworking is observed at the top of sequence 76, suggesting a considerable drop in relative sea level. It is the best candidate for 3rd-order sequence boundary Va2.

The oolitic and echinoderm-rich limestones in the last ten metres of the section are interpreted as subtidal oolite bars. Small-scale composite sequences can not be differentiated. A major facies change is observed three metres below the top of the section, where the sudden appearance of bryozoan and crinoid-rich limestones indicates another rapid opening of the depositional environments. The iron-stained surface where the change takes place is interpreted as the transgressive surface of large-scale sequence Va3. Emersion or subaerial erosion at this surface is not indicated as in other, more proximal regions of the Jura platform (Blanc 1996). The typical red-coloured facies with quartz nodules is regionally attributed to the Calcaire Roux Formation. It implies that the oolitic bars below represent an atypical Upper Chambotte Member. However, in the Salève section, no biostratigraphic markers supporting this hypothesis were found.

Discussion

Based on one section alone it is not possible to distinguish between sequence boundaries created by basin-wide or global sea-level fluctuations and those due to local effects (e.g., tectonic uplift, platform morphology). However, biostratigraphic correlation permits to compare the large-scale sequence boundaries or sequence-boundary zones identified at Salève with those observed in other shallow- and deep-water sections (Jan du Chêne et al. 1993 in the Vocontian Basin; Clavel et al. 1992 in platform and basin settings of southeastern France; Hoedemaeker 1992 in Mediterranean successions). Several of the sequence boundaries discussed here have also been recognized by Pasquier (1995), Blanc (1996), and Pasquier & Strasser (1997) on the Jura platform and in platform-to-basin correlations. Hardenbol et al. (1998) labeled the boundaries of these sequences as Be1 through Be8 for the Berriasian and Va1 to Va3 for the Lower Valanginian, and placed them in a chronostratigraphic framework (Fig. 2). The "absolute" ages attributed to these sequence boundaries are based on Gradstein et al. (1995).

Positioning and approximate timing of these large-scale sequence boundaries can now be compared with the cyclostratigraphic interpretation of the section, and a best-fit solution satisfying both sequence-stratigraphic and cyclostratigraphic approaches can be sought for.

Cyclostratigraphic interpretation

Facies evolution and the hierarchical stacking of different orders of depositional sequences suggest that relative sea-level changes of different amplitudes and frequencies played an important part in their formation. The fact that many small-scale sequences can be correlated from one section to another and over distances of up to 200 km (Strasser 1988b, 1991, 1994; Pasquier 1995; Pasquier & Strasser 1997; Hillgärtner 1998a, b) suggests an allocyclic control, i.e. sea-level fluctuations that affected at least the entire Jura platform. High-frequency sea-level fluctuations are in many cases related to insolation changes controlled by the astronomical parameters of the Earth's orbit (Milankovitch cycles: e.g., De Boer & Smith 1994; Read et al. 1995). Orbitally induced glacio-eustasy probably was present but subordinate in the Lower Cretaceous (Frakes & Francis 1988). However, varying thermal expansion of the ocean surface (Gornitz et al. 1982), thermally-induced volume changes of deep ocean water (Schulz & Schäfer-Neth 1998), waxing and waning of alpine glaciers (Fairbridge 1976), and/or release and retention of water in lakes and aquifers (Jacobs & Sahagian 1993) could easily produce sea-level fluctuations of a few metres amplitude, enough to create the observed lagoonal to peritidal sequences. Periodic input of clays and detrital quartz, periodic changes in carbonate productivity, or localized autocyclic processes were superimposed. The changes in thickness of correlated depositional sequences can be attributed to accommodation changes created by differential subsidence (Pasquier 1995).

As a working hypothesis, it is therefore assumed that the Jura platform in the Lower Cretaceous was affected by orbitally controlled sea-level fluctuations, even if complex feedback mechanisms certainly distorted the primary insolation signal (Strasser 1991). The following cyclostratigraphic interpretation of the studied section is based on the analysis of the stacking pattern, and on the bio- and chronostratigraphic framework.

At least 72 small-scale sequences have been counted or inferred between 3rd-order sequence boundaries Be1 and Va1 (Fig. 8). Be1 is dated at 144.2 (± 2.6) Ma by Hardenbol et al. (1998; based on Gradstein et al. 1995), Va1 at 136.5 Ma (Gradstein et al. 1995 indicate an error margin of ± 2.2 my for the Berriasian-Valanginian boundary at 137 Ma. The time span between these two sequence boundaries thus amounts to 7.7 ± 4.8 my. Consequently, and assuming that each small-scale sequence represents an equal length of time, one such sequence has a theoretical duration of 107 ± 67 ky. In the same interval, 19 medium-scale sequences have been identified, each with a theoretical duration of 405 ± 253 ky. Despite the large error margins of the "absolute" dating, the calculated durations of the small- and medium-scale sequences fall within the Milankovitch frequency band (Berger et al. 1989). The small-scale composite sequences may thus reflect the 100-ky cycle of eccentricity, the medium-scale sequences the 400-ky cycle of eccentricity. This hypothesis is in accordance with the observed 4:1 relationship between small-scale and medium-scale sequences (see above). On the average, 5 elementary sequences compose one small-scale composite sequence (with the exception of sequences in large-scale sequence boundary zones: Figs 5 and 7). This suggests that elementary sequences may correspond to the orbital cycle of the precession of the equinoxes, which, in the lowermost Cretaceous, had a duration of about 20 ky (Berger et al. 1989).

Thirty-two inferred 100-ky sequences have been identified between sequence boundary Be1 at the base of the Tidalites-de-Vouglans Formation and sequence boundary Be4 at the top of the Goldberg Formation (Fig. 7a, 7b). This implies a duration of 3.2 my. Hardenbol et al. (1998) equally propose 3.2 my between these two sequence boundaries (Fig. 8). In the Salève section, 3rd-order sequence boundary Be2 has been placed where the best-developed emersion features are encountered (Fig. 7b). However, according to the chart of Hardenbol et al. (1998), which is based on the comparison of many and mostly deep-water sections, this boundary should occur 1.2 my (i.e. 12 small-scale composite sequences) above sequence boundary Be1. No significant loss of accommodation is visible at Mount Salève on top of sequence 12 (Fig. 7b), but lateral correlations of this sequence show that in other sections (Yenne and Fier; Strasser 1994) there is a rapid change from dolomite-dominated small-scale sequences to calcite-dominated ones. Also, the emersion features of small-scale sequences 16 and 17 at Salève are less pronounced in Yenne and Fier. It is therefore well possible that sea-level fluctuations related to the 400-ky eccentricity cycle, and/or specific platform morphology and subsidence patterns displaced the best-marked large-scale sequence boundary.

Sequence boundary Be3 at Salève has been placed on top of thinning-up tidal-flat and lacustrine small-scale sequences, which suggest a late highstand on the long term (Figs 5 and 7b). It is followed by a rapid transgression (sequence 29). Based on the Salève section alone it cannot be decided if the "true" Be3 should be placed there, or if it is amalgamated with Be4 at the top of the Goldberg Formation. Correlation with other sections in the Swiss and French Jura (Strasser 1988b) indicates that the most restricted facies and the maximum loss of accommodation generally occurs on top of sequence 28. Hardenbol et al. (1998) attribute 141.8 Ma to Be3, instead of 141.4 as inferred from the stacking of small-scale composite sequences. Even if this difference is within the error margins of the "absolute" dating, it is also possible that the expression of sequence boundary Be3 has been shifted by a 400-ky sea-level fluctuation superimposed on a longer-term trend, or by differential subsidence.

At the top of the Goldberg Formation, below the transgressive surface forming the base of Pierre-Châtel Formation, 4 small-scale sequences are condensed at Salève, but well developed in other studied sections of the Jura platform (Strasser 1988b, 1994). Pasquier & Strasser (1997) have demonstrated that the lowstand deposits of sequence Be4 were condensed on the proximal platform for about 900 ky.

For the interval between large-scale sequence boundary Be4 at the top of Goldberg and sequence boundary Va1 at the top of the Lower Chambotte Member, 40 to 41 small-scale sequences have been observed or are inferred from lateral comparison (Fig. 8). The cyclostratigraphical analysis thus implies a time span of about 4 my, as opposed to the 4.5 my attributed by Hardenbol et al. (1998).

In the Pierre-Châtel Formation, the well marked large-scale transgressive trend with a high accommodation potential and the very mobile facies belts of tidally influenced sand dunes make it impossible to identify elementary sequences. However, modulation of the accommodation and intervals of condensation define at least 9 small-scale composite sequences mainly bounded by their maximum-flooding intervals or surfaces (37 to 45; Fig. 7c). They are laterally correlatable with well-established sequences in proximal areas of the platform (Pasquier 1995). In the covered interval at the top of the Formation, 3 small-scale composite sequences are inferred from lateral comparison. This implies a duration of 1.2 my for the Pierre-Châtel Formation.

The Vions Formation generally shows a much lower accommodation and, therefore, well-marked high-frequency variations. In several intervals of the section repetitive small-scale emersions are observed. They delimit sequence-boundary zones where superposition of several orders of relative sea-level fall are translated into multiplied small-scale sequence boundaries (Fig. 6). Sequence-boundary zone Be6 comprises sequences 51 to 53, which show low accommodation and repetitive palaeosol formation (Fig. 7d). Higher up in the section, major losses in accommodation marked by subaerial exposure or intertidal facies occur at the tops of sequences 55, 59, 62, and 65. These prominent surfaces are interpreted as the limits of medium-scale composite sequences with inferred time durations of 400 ky. Sequence-boundary zone Be7 corresponds to a regionally observed maximum regression, and sequence-boundary zone Be8 shows emersions marked by palaeosols and coal horizons. Important condensation and erosion probably occurred in these zones and may explain that only three small-scale composite sequences are identified in medium-scale sequences 16 and 17 (Fig. 7d). The cyclostratigraphically deduced duration between sequence boundaries Be5 and Be8 thus is 1.8 to 2.1 my, depending on the positioning of the "true" sequence boundaries within their zones, and including the probably condensed small-scale composite sequences.

In the Lower Chambotte Member (between Be8 and Va1), 7 to 8 small-scale composite sequences are identified, which commonly show vadose diagenesis at their tops. This implies a duration of about 800 ky, which is confirmed by correlation with deeper-water sections in the Vocontian Trough (Hillgärtner 1998b).

The interval between sequence boundaries Va1 and Va3 poses problems for a cyclostratigraphic interpretation. The mobile high-energy facies with a generally elevated accommodation indicates a strong transgressive trend on a higher order. This causes condensed intervals and attenuated small-scale regressive trends, which hindered the development of a well-defined stacking pattern.

Discussion

The cyclostratigraphic interpretation, based on the assumption that the observed hierarchical stacking of elementary, small-scale, and medium-scale depositional sequences is related to sea-level fluctuations controlled by orbital insolation cycles, appears to be fairly consistent with the general time framework given by Hardenbol et al. (1998). Unfortunately, the sedimentary record is not complete enough and the biostratigraphic dating not precise enough for the establishment of a cyclostratigraphical timescale (e.g., House & Gale 1995). Nevertheless, the sequence stratigraphic and cyclostratigraphic interpretations presented above allow to better explain the sedimentological evolution of the studied section.

The position of the Salève section on the external part of the shallow Jura platform, the slow changes of accommodation on the longer term (especially in the Berriasian), and the high carbonate production keeping pace with increasing water depth permitted that most high-frequency sea-level fluctuations could create discontinuity surfaces and facies changes defining the different orders of depositional sequences. Where low accommodation predominated (during deposition of the Tidalites-de-Vouglans, Goldberg, and Vions Formations), the 20-ky cycle was recorded in the elementary sequences (although part of the 20 ky may have been spent in non-deposition, reworking, and/or erosion; Strasser 1994). Where accommodation generally was higher (Pierre-Châtel and Chambotte Formations), the amplitudes of the 20-ky sea-level cycle were not always big enough to create bounding surfaces, and the 20-ky sequences are not recorded or ill defined. On the other hand, if accommodation was very low such as around large-scale sequence boundaries, some elementary sequences were not deposited at all, deposited and eroded again, or highly condensed (examples in Fig. 5). The sequences related to the 100-ky cyclicity generally are well expressed, even if some of their elementary sequences may have been lost when accommodation was low. On the other hand, these small-scale sequences may be difficult to distinguish when relative sea-level rises were fast such as during deposition of the Lower and Upper Chambotte Members. Stacking related to obliquity cycles (ca. 38 ky in the lowermost Cretaceous; Berger et al. 1989) could not be identified.

All widely recognized 3rd-order sequence boundaries of the Berriasian and the Lower Valanginian (Hardenbol et al. 1998) have been identified in the Salève section. However, it appears through the cyclostratigraphical analysis that some of these sequences correspond to the 400-ky cycle of eccentricity (medium-scale sequences 8 and 13, and medium-scale sequence 14 up to the base of sequence-boundary zone Be7; Fig. 7). The "beat" of the 400-ky orbital cyclicity was at times strong enough to create regionally correlatable sequences (Strasser 1994; Hillgärtner 1998b). Also, it is interesting to note that this 400-ky cyclicity was in many cases responsible for important facies changes (Figs 7 and 8).

Due to the superposition of short-term sea-level fluctuations over a longer-term (3rd-order) trend, mostly zones of sequence boundaries rather than sharply defined unique surfaces are created. In the same way, maximum-flooding surfaces of large-scale sequences are not necessarily developed, and only relatively deepest facies and thick beds indicate maximum accommodation potential. True "systems tracts" can only be inferred if a correlation with slope and basinal sections has been established (Pasquier & Strasser 1997).

Features testifying to tectonic activity during the Berriasian and Early Valanginian have been described in many areas along the north-western Tethyan margin (e.g., Boillot et al. 1984, De Graciansky & Lemoine 1988). They are related to the Late Cimmerian phase of rifting of the Atlantic Ocean (Ziegler 1990, Sinclair et al. 1994). Abrupt changes in subsidence rate and block faulting accentuated or attenuated the effects of sea-level change in the sedimentary record, and differential uplift probably was responsible for the hiatus around Be4 in the Salève section. However, it is important to note that the signal of longer-term eustatic sea-level changes still is clearly recorded.

Conclusions

The studied section of Berriasian to Lower Valanginian peritidal and lagoonal carbonate-dominated sediments exhibits a stacking of elementary, small-scale, medium-scale, and large-

Formations Members	Sequence boundaries	Ages according to Hardenbol et al. (1998)	Estimated time intervals according to Hardenbol et al. (1998)	Small-scale sequences between SBs	Medium-scale sequences between SBs	Inferred time spans between SBs
	Va1	136.5 (±2.2)				
Lower Chambotte			900 ka	7 (or 8)	2	800 ka
	Be8	137.4				
Vions			700 ka	10 (or 6)	3 (or 2)	1.6 Ma
	Be7	138.1				
			500 ka	4 (or 8)	1 (or 2)	
	Be6	138.6				
			700 ka	3	1	400 ka
	Be5	139.3				
Pierre-Châtel Hiatus			1.7 Ma	3 inferred + 9 observed + 4 inferred	3 observed + 1 inferred	1.6 Ma
	Be4	141.0				
Goldberg			800 ka	4	1	400 ka
	Be3	141.8				
			1.2 Ma	12	3	1.2 Ma
	Be2	143.0				
Vouglans			1.2 Ma	16	4	1.6 Ma
	Be1	144.2 (±2.6)				

Fig. 8. Comparison of time represented in the studied section. For discussion refer to text (SB: sequence boundary).

scale depositional sequences. The rapid facies changes and clay input, which allow to define such sequences, are attributed to low-amplitude sea-level fluctuations of different frequencies. High-frequency sea-level fluctuations were superimposed on a longer-term trend that determined the general facies development. Many longer-term sea-level drops and rises therefore did not create unique sequence boundaries or maximum-flooding surfaces, but rather zones expressing minimum or maximum accommodation, respectively. The general time framework as well as the hierarchical stacking of an average of 5 elementary sequences into a small-scale sequence, and of 4 small-scale sequences into a medium-scale sequence suggest that the high-frequency sea-level changes were controlled by climatic changes in tune with orbital (Milankovitch) cycles.

Biostratigraphic control allows to compare most large-scale sequence boundaries or sequence-boundary zones with the 3rd-order sequence boundaries recognized by Hardenbol et al. (1998). Assuming that the elementary sequences seen in the outcrop correspond to the 20-ky cycles of the precession of the equinoxes, the small-scale sequences to the 100-ky orbital eccentricity cycle, and the medium-scale sequences to the 400-ky eccentricity cycle, a time span of 7.2 to 7.6 my is inferred between sequence boundaries Be1 and Va1. For the same stratigraphic interval, Hardenbol et al. (1998), based on Gradstein et al. (1995), propose 7.7 ± 4.8 my.

When accommodation is moderate on the shallow platform, the 20-ky, 100-ky, and 400-ky cyclicities are well expressed. When a longer-term transgressive trend is predominant, the 20-ky and sometimes also the 100-ky cyclicities are lost. When accommodation is very low, elementary and, locally, small-scale sequences may not be deposited, condensed, or eroded. However, despite of such gaps within the depositional sequences, the general stacking pattern is preserved. The medium-scale, 400-ky cycles are responsible for many important facies changes, and several of the regionally recognized 3rd-order sequence boundaries coincide with medium-scale sequence boundaries.

Differential subsidence related to the Late Cimmerian tectonic phase influenced the Jura platform, but did not preclude the recording of the longer-term sea-level changes. Localized tectonic uplift, however, sometimes created rapid loss of accommodation and led to condensation, non-deposition, or erosion.

This study shows that, through detailed analysis of facies and stacking pattern, the high- to low-frequency and high- to low-amplitude accommodation changes through time can be reconstructed. If a Milankovitch pattern is detected and the duration of the high-frequency cycles is confirmed by dating of chronostratigraphic tie points, a very detailed time framework can be established. Combining high-resolution sequence stratigraphy and cyclostratigraphy thus allows to better monitor the complex sedimentary processes affecting shallow depositional environments.

Acknowledgements

We thank Jean-Bruno Pasquier and Bernard Pittet for long and fruitful discussions in the field, and Pierre-Olivier Mojon for communicating data on charophyte-ostracod assemblages. The thoughtful and constructive reviews by Pierre-Charles de Graciansky and Hubert Arnaud as well as the editorial help by Jürgen Remane greatly improved the manuscript. This study was supported by grants of the Swiss National Science Foundation (No. 20–37386.93 and 20–46625.96).

REFERENCES

Berger, A., Loutre, M.F. & Dehant, V. 1989: Astronomical frequencies for pre-Quaternary palaeoclimate studies. Terra Nova 1, 474–479.

Bernier, P. 1984: Les formations carbonatées du Kimméridgien et du Portlandien dans le Jura méridional. Stratigraphie, micropaléontologie et sédimentologie. Doc. Lab. Géol. Lyon 92, 803 pp.

BLANC, E. 1996: Transect plate-forme – bassin dans les séries carbonatées du Berriasien supérieur et du Valanginien inférieur (domaines jurassien et nord vocontien); Chronostratigraphie et tranferts des sédiments. Géologie Alpine 25, 312 pp.

BOILLOT, G., MONTADERT, L., LEMOINE, M. & BIJU-DUVAL, B. 1984: Les marges continentales actuelles et fossiles autour de la France. Masson, Paris, 342 pp.

BOND, G.C., DEVLIN, W.J., KOMINZ, M.A., BEAVAN, J. & MCMANUS, J. 1993: Evidence of astronomical forcing of the Earth's climate in Cretaceous and Cambrian times. Tectonophysics 222, 295–315.

CAROZZI, A.V. 1948: Etude stratigraphique et micrographique du Purbeckien du Jura suisse. Kündig, Genève, 175 pp.

– 1953: A propos de la limite Kimméridgien–Portlandien au Grand-Salève (Haute-Savoie). Cah. géol. Thoiry 13, 153–155.

– 1954: Le Jurassique supérieur récifal du Grand-Salève, essai de comparaison avec les récifs coralliens actuels. Eclogae geol. Helv. 47, 373–376.

– 1955: Sédimentation récifale rythmique dans le Jurassique supérieur du Grand-Salève. Geol. Rdsch. 43, 433–446.

CLAVEL, B., CHAROLLAIS, J., BUSNARDO, R. & LE HEGARAT, G. 1986: Précisions stratigraphiques sur le Crétacé inférieur basal du Jura méridional. Eclogae geol. Helv. 79, 319–341.

CLAVEL, B., BUSNARDO, R., CHAROLLAIS, J. & SCHROEDER, R. 1992: Sequence stratigraphy: a paleontological approach for the Lower Cretaceous. Abstr. Colloque CNRS-IFP, Sequence Stratigraphy of European Basins, Dijon, 478–479.

D'ARGENIO, B., FERRERI, V., AMODIO, S. & PELOSI, N. 1997: Hierarchy of high-frequency orbital cycles in Cretaceous carbonate platform strata. Sed. Geol. 113, 169–193.

DE BOER, P.L. & SMITH, D.G. (Eds) 1994. Orbital Forcing and Cyclic Sequences. Spec. Publ. Int. Assoc. Sedimentol. 19, 559 pp.

DECONINCK, J.-F. & STRASSER, A. 1987: Sedimentology, clay mineralogy and depositional environment of Purbeckian green marls (Swiss and French Jura). Eclogae geol. Helv. 80, 753–772.

DE GRACIANSKY, P.-C. & LEMOINE, M. 1988: Early Cretaceous extensional tectonics in the southwestern French Alps: a consequence of North-Atlantic rifting during Tethyan spreading. Bull. Soc. géol. France (8) 4, 733–737.

DÉTRAZ, H. & MOJON, P.-O. 1989: Evolution paléogéographique de la marge jurassienne de la Téthys du Tithonique-Portlandien au Valanginien: corrélations biostratigraphique et séquentielle des faciès marins à continentaux. Eclogae geol. Helv. 82, 37–112.

DEVILLE, Q. 1991: Stratigraphie, sédimentologie et environnements de dépôts, et analyse séquentielle dans les terrains entre le Kimméridgien supérieur et le Valanginien du Mont-Salève (Haute-Savoie, France). Unpubl. PhD Thesis, Geneva, 141 pp.

FAIRBRIDGE, R.W. 1976: Convergence of evidence on climatic change and ice ages. Ann. N.Y. Acad. Sci. 91, 542–579.

FRAKES, L.A. & FRANCIS, J.E. 1988: A guide to Phanerozoic cold polar climates from high-latitude ice-rafting in the Cretaceous. Nature 333, 547–549.

GINSBURG, R.N. 1971: Landward movement of carbonate mud: new model for regressive cycles in carbonates (abstract). Bull. Amer. Assoc. Petrol. Geol. 55, 340.

GOLDHAMMER, R.K., DUNN, P.A. & HARDIE, L.A. 1990: Depositional cycles, composite sea-level changes, cycle stacking patterns, and the hierarchy of stratigraphic forcing: Examples from Alpine Triassic platform carbonates. Bull. geol. Soc. Amer. 102, 535–562.

GOLDHAMMER, R.K., OSWALD, E.J. & DUNN, P.A. 1994: High-frequency, glacio-eustatic cyclicity in the Middle Pennsylvanian of the Paradox Basin: an evaluation of Milankovitch forcing. In: Orbital Forcing and Cyclic Sequences (Ed. by DE BOER, P.L. & SMITH, D.G.). Spec. Publ. Int. Assoc. Sedimentol. 19, 243–283.

GORIN, G.E., SIGNER, C. & AMBERGER, G. 1993: Structural configuration of the western Swiss Molasse Basin as defined by reflection seismic data. Eclogae geol. Helv. 86, 693–716.

GORNITZ, V., LEBEDEFF, S. & HANSEN, J. 1982: Global sea-level trend in the past century. Science 215, 1611–1614.

GRADSTEIN, F.M., AGTERBERG, F.P., OGG, J.G., HARDENBOL, J., VAN VEEN, P., THIERRY, J. & HUANG, Z. 1995: A Triassic, Jurassic and Cretaceous time scale. In: Geochronology, Time Scales and Global Stratigraphic Correlation (Ed. by BERGGREN, W.A., KENT D.V., AUBRY, M.P. & HARDENBOL, J.). Spec. Publ. Soc. Sed. Geol. 54, 95–126.

HÄFELI, C. 1966: Die Jura/Kreide-Grenzschichten im Bielerseegebiet (Kt. Bern). Eclogae geol. Helv. 59, 565–696.

HANDFORD, C.R. & LOUCKS, R.G. 1993: Carbonate depositional sequences and systems tracts – responses of carbonate platforms to relative sea-level changes. In: Carbonate Sequence Stratigraphy (Ed. by LOUCKS, R.G. & SARG, J.F.). Mem. Amer. Assoc. Petrol. Geol. 57, 3–41.

HAQ, B.U., HARDENBOL, J. & VAIL, P.R. 1987: Chronology of fluctuating sea levels since the Triassic. Science 235, 1156–1167.

HARDENBOL, J., THIERRY, J., FARLEY, M.B., JACQUIN, T., DE GRACIANSKY, P.-C. & VAIL, P.R. 1998: Cretaceous chronostratigraphy. In: Sequence Stratigraphy of European Basins (Ed. by DE GRACIANSKY, P.-C., HARDENBOL, J., JACQUIN, T., VAIL, P.R. & FARLEY, M.B.). Spec. Publ. Soc. Sed. Geol. (in print).

HILLGÄRTNER, H. 1998a: Discontinuity surfaces on a shallow-marine carbonate platform (Berriasian, Valanginian, France and Switzerland). J. sed. Res. (in print).

– 1998b: The evolution of the French Jura platform during the Late Berriasian to Early Valanginian: controlling factors and timing. PhD Thesis Univ. Fribourg (in print).

HOEDEMAEKER, P.J. 1992: Lower Cretaceous ammonite biostratigraphy and sequence stratigraphy. Abstr. Colloque CNRS-IFP, Sequence Stratigraphy of European Basins, Dijon, 278–279.

HOUSE, M.R. & GALE, A.S. (Eds) 1995: Orbital Forcing Timescales and Cyclostratigraphy. Geol. Soc. Spec. Publ. 85, 210 pp.

JACOBS, D.K. & SAHAGIAN, D.L. 1993: Climate-induced fluctuations in sea level during non-glacial times. Nature 361, 710–712.

JAN DU CHÊNE, R., BUSNARDO, R., CHAROLLAIS, J., CLAVEL, B., DECONINCK, J.-F., EMMANUEL, L., GARDIN, S., GORIN, G., MANIVIT, H., MONTEIL, E., RAYNAUD, J.-F., RENARD, M., STEFFEN, D., STEINHAUSER, N., STRASSER, A., STROHMENGER, C. & VAIL, P.R. 1993: Sequence-stratigraphic interpretation of Upper Tithonian – Berriasian reference sections in South-East France: a multidisciplinary approach. Bull. Centres Rech. Explor.-Prod. Elf Aquitaine 17, 151–181.

JOACHIMSKI, M.M. 1994: Subaerial exposure and deposition of shallowing upward sequences: evidence from stable isotopes of Purbeckian peritidal carbonates (basal Cretaceous), Swiss and French Jura Mountains. Sedimentology 41, 805–824.

JOUKOWSKY, E. & FAVRE, J. 1913: Monographie géologique et paléontologique du Salève (Haute-Savoie, France). Mém. Soc. Phys. Hist. nat. Genève 37/4, 295–523.

LE HÉGARAT, G. 1971: Le Berriasien du Sud-Est de la France. Doc. Lab. Géol. Fac. Sci. Lyon 43, 567 pp.

– 1980: Berriasien. In: Les étages français et leurs stratotypes (Ed. by CAVELIER, J. & ROGER, J.). Mém. Bur. Rech. géol. min. 109, 96–105.

LE HÉGARAT, G. & REMANE, J. 1968: Tithonique supérieur et Berriasien de l'Ardèche et de l'Hérault: corrélation des ammonites et des calpionelles. Geobios 1, 7–70.

LOEBLICH, A.R.Jr. & TAPPAN, H. 1988: Foraminiferal Genera and their Classification. Van Nostrand Reinhold, New York, 970 pp.

LOMBARD, A. 1967: Le Salève. In: Guide géologique de la Suisse 2 (Ed. by Soc. Géol. Suisse). Wepf, 54–57.

– 1976: Les couches de la Corraterie-Vions au Grand Salève (Haute-Savoie): faux nodules ou phacosomes. Arch. Sci. Genève 29, 201–213.

MAILLARD, G. 1884: Etude sur l'étage purbeckien dans le Jura. Thesis Univ. Zurich, 77 pp.

MITCHUM, R.M. Jr. & VAN WAGONER, J.C. 1991: High-frequency sequences and their stacking patterns: sequence-stratigraphic evidence of high-frequency eustatic cycles. Sed. Geol. 70, 131–160.

MOJON, P.-O. 1988: Contribution à l'étude micropaléontologique, paléoécologique et biostratigraphique des faciès "portlandiens" et "purbeckiens" (limite Jurassique-Crétacé) du Salève (Haute-Savoie, France). Arch. Sci. Genève 41, 99–102.

MOJON, P.-O. & STRASSER, A. 1987: Microfaciès, sédimentologie et micropaléontologie du Purbeckien de Bienne (Jura suisse occidental). Eclogae geol. Helv. 80, 37–58.
MONTAÑEZ, I.A. & OSLEGER, D.A. 1993: Parasequence stacking patterns, third-order accommodation events, and sequence stratigraphy of Middle to Upper Cambrian platform carbonates, Bonanza King Formation, southern Great Basin. In: Carbonate Sequence Stratigraphy (Ed. by LOUCKS, R.G. & SARG, J.F.). Mem. Assoc. Petrol. Geol. Mem. 57, 305–326.
OSLEGER, D.A. 1991: Subtidal carbonate cycles: Implications for allocyclic vs. autocyclic controls. Geology 19, 917–920.
PASQUIER, J.-B. 1995: Sédimentologie, stratigraphie séquentielle et cyclostratigraphie de la marge nord-thétysienne au Berriasien en Suisse occidentale (Jura, Helvétique et Ultrahelvétique; comparaison avec les séries de bassin des domaines vocontien et subbriançonnais). Unpubl. PhD Thesis, Fribourg, 274 pp.
PASQUIER, J.-B. & STRASSER, A. 1997: Platform-to-basin correlation by high-resolution sequence stratigraphy and cyclostratigraphy (Berriasian, Switzerland and France). Sedimentology 44, 1071–1092.
PERLMUTTER, M.A., MATTHEWS, M.A. 1989: Global cyclostratigraphy – a model. In: Quantitative Dynamic Stratigraphy (Ed. by CROSS, T.A.). Prentice Hall, Englewood Cliffs, 233–260.
PITTET, B. & STRASSER, A. 1998: Long-distance correlations by sequence stratigraphy and cyclostratigraphy: examples and implications (Oxfordian from the Swiss Jura, Spain, and Normandy). Geol. Rdsch. 86, 852–874.
POSAMENTIER, H.W., JERVEY, M.T. & VAIL, P.R. 1988: Eustatic controls on clastic deposition I – conceptual framework. In: Sea-Level Changes: an Integrated Approach (Ed. by WILGUS, C.K., HASTINGS, B.S., KENDALL, C.G.ST.C., POSAMENTIER, H.W., ROSS, C.A. & VAN WAGONER, J.C.). Soc. Econ. Pal. Min. Spec. Publ. 42, 109-124.
PRATT, B.R. & JAMES, N.P. 1986: The St George Group (Lower Ordovician) of western Newfoundland: tidal flat island model for carbonate sedimentation in shallow epeiric seas. Sedimentology 33, 313–343.
READ, J.F. & GOLDHAMMER R.K. 1988: Use of Fischer plots to define third-order sea-level curves in Ordovician peritidal cyclic carbonates, Appalachians. Geology 16, 895–899.
READ, J.F., KERANS, C., WEBER, L.J., SARG, J.F. & WRIGHT, F.M., 1995: Milankovitch sea-level changes, cycles, and reservoirs on carbonate platforms in greenhouse and icehouse worlds. Soc. Econ. Paleont. Miner. Short Course, 35.
REMANE, J. 1985: Calpionellids. In: Plankton Stratigraphy (Ed. by BOLLI, H.M., SAUNDERS, J.B. & PERCH-NIELSEN, K.). Univ. Press Cambridge, 555–572.
SCHLAGER, W. 1993: Accommodation and supply – a dual control on stratigraphic sequences. Sed. Geol. 86, 111–136.
SCHULZ, M. & SCHÄFER-NETH, C. 1998: Translating Milankovitch climate forcing into eustatic fluctuations via thermal deep water expansion: a conceptual link. Terra Nova 9, 228–231.
SINCLAIR, I.K., SHANNON, P.M., WILLIAMS, B.P.J., HARKER, S.D. & MOORE, J.G. 1994: Tectonic control on sedimentary evolution of three North Atlantic borderland Mesozoic basins. Basin Res. 6, 193–217.
STEINHAUSER, N. & LOMBARD, A. 1969: Définition de nouvelles unités lithostratigraphiques dans le Crétacé inférieur du Jura méridional (France). C.R. Soc. Phys. Hist. nat. Genève 4, 100–113.
STRASSER, A. 1988a: Enregistrement sédimentaire de cycles astronomiques dans le Portlandien et Purbeckien du Salève (Haute-Savoie, France). Arch. Sci. Genève 41, 85–97.
– 1988b: Shallowing-upward sequences in Purbeckian peritidal carbonates (lowermost Cretaceous, Swiss and French Jura Mountains). Sedimentology 35, 369–383.
– 1991: Lagoonal-peritidal sequences in carbonate environments: autocyclic and allocyclic processes. In: Cycles and Events in Stratigraphy (Ed. by EINSELE, G., RICKEN, W. & SEILACHER, A.). Springer-Verlag, 709–721.
– 1994: Milankovitch cyclicity and high-resolution sequence stratigraphy in lagoonal-peritidal carbonates (Upper Tithonian – Lower Berriasian, French Jura Mountains). In: Orbital Forcing and Cyclic Sequences (Ed. by DE BOER, P.L. & SMITH, D.G.). Spec. Publ. Int. Ass. Sediment. 19, 285–301.
STRASSER, A. & DAVAUD, E. 1983: Black pebbles of the Purbeckian (Swiss and French Jura): lithology, geochemistry and origin. Eclogae geol. Helv. 76, 551–580.
TIPPER, J.C. 1997: Modeling carbonate platform sedimentation – lag comes naturally. Geology 25, 495–498.
VAIL, P.R., AUDEMARD, F., BOWMAN, S.A., EISNER, P.N. & PEREZ-CRUZ, C. (1991): The stratigraphic signatures of tectonics, eustasy and sedimentology – an overview. In: Cycles and Events in Stratigraphy (Ed. by EINSELE, G., RICKEN, W. & SEILACHER, A.). Springer-Verlag, 617–659.
VAN WAGONER, J.C., MITCHUM, R.M., CAMPION, K.M. & RAHMANIAN, V.D. 1990: Siliciclastic Sequence Stratigraphy in Well Logs, Cores, and Outcrops. Am. Ass. Petrol. Geol. Methods in Explor. 7, 55 pp.
ZANINETTI, L., CHAROLLAIS, J., CLAVEL, B., DECROUEZ, D., SALVINI-BONNARD, G. & STEINHAUSER, N. 1988: Quelques remarques sur les fossiles du Salève (Haute-Savoie, France). Arch Sci. Genève 41, 43–63.
ZIEGLER, P.A. 1990: Geological Atlas of Western and Central Europe (2nd ed.). Shell Int. Petrol. Maatschappij B.V., 239 pp.

Manuscript received January 7, 1998
Revision accepted October 24, 1998